Receiver Calorimeter of Fast Atom Beam Injector in Megawatt Range

V. Kh. Amirov[a,*], T. D. Akhmetov[a,b], A. I. Gorbovskiy[a], P. P. Deychuli[a], A. A. Ivanov[a], V. A. Kapitonov[a], and I. V. Shikhovtsev[a,b]

[a] Budker Institute of Nuclear Physics, Siberian Branch, Russian Academy of Sciences, Novosibirsk, 630090 Russia
[b] Novosibirsk State University, Novosibirsk, 630090 Russia
***e-mail: V.Kh.Amirov@inp.nsk.su**

Abstract—The receiver calorimeter (RC) is one of the main elements of the beam path of an atomic beam injector with ballistic focusing. A water-cooled RC developed for an injector of a focused beam of fast deuterium atoms with a beam power of more than 1 MW and pulse duration of 2 s [1] installed at the variable configuration tokamak (TCV) in Lausanne (Switzerland) is considered. The design of the RC includes receiving plates with liquid flow swirlers installed in them to enhance heat transfer and pipe-in-pipe collectors of water inlet and water outlet that provide the movement into a vacuum. These technical solutions made it possible to achieve good energy efficiency of the device with very small overall dimensions and mass flow of the coolant. The design of the main elements of the calorimeter is described. The results of simulation of the coolant flow and heat transfer and some experimental data are presented.

INTRODUCTION

Injection of high-power beams of fast atoms is one of the effective methods for heating plasma in magnetically confined thermonuclear traps and generating current in them. The fast atom beam injector consists of the main systems (except for the power supply and control systems). They are a source of positive or negative ions depending on the purpose of the injector and the required particle energy that ensures the generation of an ion beam and its focusing and acceleration to a given energy; a neutralizer designed to convert beam ions into atoms; a bending magnet separating the beam of fast atoms from the residual ions; a receiver of residual ions; a neutral beam receiver calorimeter (RC) designed for absorbing the beam energy under preparing for a working shot into a plasma trap and for measuring the beam power and its spatial profile; and a pumping system that maintains acceptable vacuum conditions during the operation of the injector.

The receiver calorimeter is the last element in the beam path before the input port of the plasma facility. In practice, it serves to absorb the beam power during the training of the grid unit of the ion source and to measure the beam power and its profile and determine its spatial position relative to the axis of the beam path. Thus, a significant part of the shots of the injector (training of the high-voltage strength of the ion optical system (IOS), tuning, and testing) is carried out not into the plasma of the facility, but when operating in the autonomous mode.

The RCs can be located inside the vacuum volume of the injector or have their own vacuum chamber.

According to the method of moving into the working position, calorimeters are sliding, rotary (rotation around a fixed axis), submersible, and fixed (if necessary, they are mounted in the beam path and then dismantled).

As a rule, the receiving part of the calorimeter is made in the form of a system of pipes or plates, and cooling channels are inside of the pipes and plates. To cool the receiving elements of the calorimeter, water is used in most designs, although other liquids or gases can be used.

As the power of fast atom beam injectors increases, the RC requirements increase. The most important parameter that determines the RC design (the power density on the RC plates, which reaches values of tens of kW cm^{-2}) increases with increasing injection power. The duration of the injection pulse in large research facilities is several seconds or more, so that the conditions for absorption of the beam by the calorimeter are usually close to stationary. All these factors lead to significant heating of the receiving elements, which must
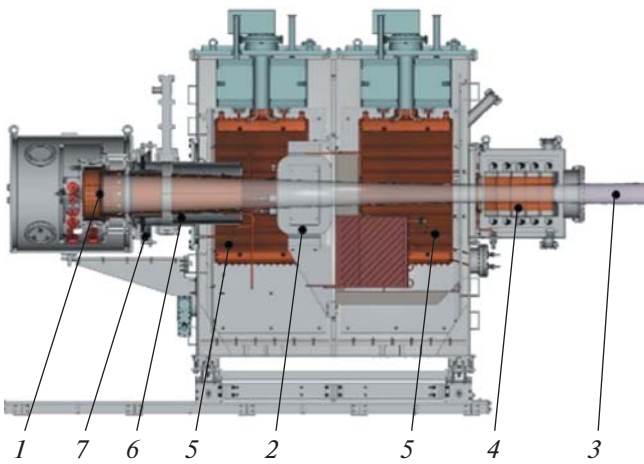
Fig. 1. Layout of the fast atom injector. (*1*) Ion source (HF driver, ion optical system), (*2*) bending magnet, (*3*) beam of fast atoms, (*4*) receiver calorimeter, (*5*) cryopumps, (*6*) neutralizer, and (*7*) adjusting unit.

be intensely cooled. It is important to simulate the RC operation. This allows one to identify negative factors and eliminate them at the design stage or mitigate their consequences. It is necessary to simulate and then organize the flow of the coolant in such a way as to avoid a large number of local resistances (sharp increase in the cross section, turns, flow swirls, and reverse flow zones), which will allow avoiding high coolant flow rates and increased loads on the supply system. In addition, it is important to ensure the required mode of heat exchange between the receiving element and the coolant. This will make it possible to avoid local overheating and, as a result, disruption of heat removal and destruction of receiving device elements of the calorimeter.

In this case, the RC receiving plates were cooled with water. The most important indicator of the RC operation mode is the intensity of heat transfer. The intensity of heat transfer is characterized by the heat transfer coefficient. It is a function of several variables and strongly depends on the nature of the coolant flow. The nature of the coolant flow under real conditions cannot be considered as a self-similar case (problem). It is significantly dependent on the architecture of the water main. The main task is to increase the heat transfer coefficient in every possible way. One of the ways to increase the heat transfer coefficient is the use of heat transfer enhancers [2]. Heat transfer enhancers make it possible to increase the intensity of heat transfer between the channel wall and the coolant flow by influencing the flow.

TCV NEUTRAL BEAM INJECTOR

A charge-exchange injector of a focused beam of fast deuterium atoms with energy of 30 keV, power of 1 MW, and duration of 2 s was developed at the Budker

Institute of Nuclear Physics, Siberian Branch, Russian Academy of Sciences, for plasma heating in the TCV (Lausanne, Switzerland). A multislit three-electrode ion optical system with spherical electrodes and an emission surface 250 mm in diameter is used in the ion source of the injector to produce the beam. The focal length of the ion optical system is 4.1 m.

The layout of the charge-exchange injector of a powerful focused beam of fast deuterium atoms for plasma heating in the TCV is shown in Fig. 1. The ion source produces a focused beam of deuterium ions with a current of up to 45 A and energy of up to 30 keV. The ion beam is then recharged into atoms in the gaseous target of the neutralizer. Unrecharged ions are deflected by a magnet and enter a water-cooled receiver. The injection tank is pumped out by four cryopumps. An expandable calorimeter is docked at the outlet of the injection tank to measure the power of the resulting beam of fast atoms. Main parameters of the injector are as follows:

Beam power through the TCV port, MW	1.00−1.05
Beam energy stability, %	Better than ±5
Nominal beam energy, keV	30 ± 5%
Ripple of energy, %	Less than ±5
Basic atomic component	Deuterium
Additional atomic component	Hydrogen
Neutral beam duration (without modulation and power sweep), s	2
Total fractional energy of neutral beam (power), %	≥65
Heavy impurities (power), %	<0.5 of the basic component
Beam power range, %	30−100 of nominal power
Beam energy range, keV	15−35

A calorimeter that completely covers the beam in the desired zone and effectively cools the receiving elements during operation is necessary to absorb the beam with specified parameters. To determine the main parameters (power density distribution on the calorimeter plates and required water flow) and the preliminary design scheme of the device, it is necessary to calculate the expected power density on the receiving plates.

Calculations of Power Density on RC Plates

The focal lengths of the ion optical system of the injector and the angular divergences across and along the slits of the grids were determined experimentally from the measured width and height of the beam at the $1/e$ level at two distances from the ion optical system on a beam bench at the Budker Institute of Nuclear

Physics [3]. The numerical values of these quantities were then confirmed by optical measurements of the temperature distribution of the surface of a flat tungsten plate heated by a neutral beam in the injection tract of the TCV. After neutralization of the ion beam accelerated by the grid system of the injector, the power of the beam of deuterium atoms was 1.30 MW. The ion optical system consisted of round electrodes 250 mm in diameter with multislit holes. The focal length and angular divergence were $F_x = 376$ cm and $\alpha_x = 24.4$ mrad across the slits (horizontally in the tokamak system) and $F_y = 398$ cm and $\alpha_y = 10.3$ mrad along the slits (vertically).

For thermal calculations of the calorimeter, it is necessary to determine the power flux density of the atomic beam along the normal to the surface of its receiving plates shown in Fig. 2.

The beam power flux density has a maximum on the axis and decreases with distance from it. The code from [4] was used to calculate the power passing at the point $P(x, y, z)$ through a unit area perpendicular to the beam axis. The power density distribution is shown in Fig. 3.

The maximum power density directly in front of the calorimeter diaphragm ($z = 225.4$ cm) on the beam axis is $P_{dia} = 11.56$ kW cm^{-2}. The power density on the calorimeter plate (rear left) at the point with coordinates of $z = 225.4 + 44.0 = 269.4$ cm, $x = 0.3$ cm, and $y = 0$ is $P_{cal} = 13.52$ kW cm^{-2}. The power density along the normal to the plate surface is $P_{normal} = P_{cal}\sin\theta = 13.52 \times 0.14 = 1.88$ kW cm^{-2}. With consideration of the error of the initial power of the neutral beam of $\pm 2\%$, the error of the normal power density is $P_{normal} = 1.88 \pm 0.04$ kW cm^{-2}. The power densities for the calculated points corresponding to the locations of the diaphragms were determined in a similar way. The data of calculations are given in Table 1.

The characteristic size at which the beam power density changes along the plate is much larger than the plate thickness. Therefore, the heat conduction problem in the first approximation can be considered one-dimensional; i.e., the heat flux along the plate can be neglected in comparison with the flux from the plate surface to the cooling zone. Then, the temperature at any depth inside the calorimeter plate is determined by the balance between the local heating power density on the plate surface and the heat flux to the zone cooled by the liquid. Consequently, the temperature change of thermocouples $\Delta T = T - T_0$ must be proportional to the local normal power density of the neutral beam $\Delta T \propto P_n$.

Figure 4 shows a graph of the distribution of the calculated normal power density in the area of the upper row of thermocouples on each plate of the calorimeter.

It should be taken into account that not the entire beam power incident on the calorimeter plate is com-
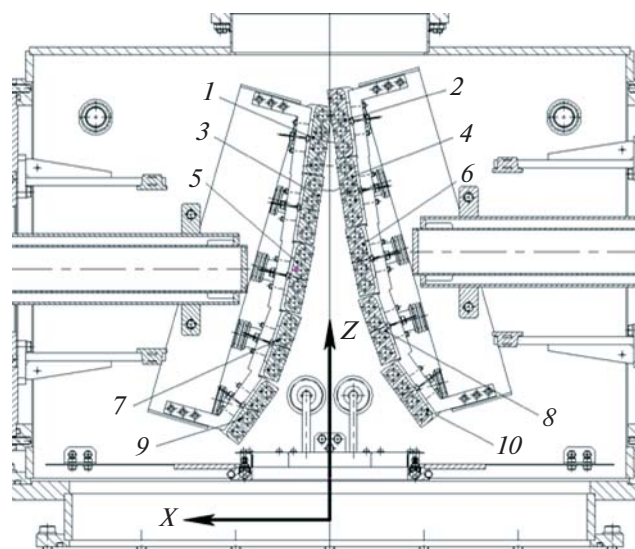

Fig. 2. Cross section of the calorimeter in the horizontal plane. The plates of the calorimeter are arranged vertically. The diaphragm of the calorimeter is shown at the bottom of the drawing. The neutral beam propagates along the z axis. The x–z coordinate plane is horizontal in the tokamak system; the y axis is directed vertically upwards. Numbers of calorimeter plates (*1–10*) are shown.

pletely absorbed. Part of the energy of the original deuterium atoms is carried away by them owing to the reflection of the atoms from the plate. In addition, the energy of the beam atoms is partially spent on the sputtering of the plate material [5, 6]. The fraction of reflected energy and the fraction of energy for sputtering of the plate material depend on the mass and energy of the incident particles, the angle of incidence, and the surface material.

In our case, the energy of deuterium atoms is 27 keV, and the angle of incidence of atoms on the calorimeter plates (the angle from the normal to the surface) is from 54° for the outermost plates to 82° for the central plates (see Fig. 2 and Table 2). The fraction of reflected energy can be measured from numerical calculations using the TRIM code [5]. The energy reflection coefficient (the ratio of the mean energy of atoms reflected at any angle to the energy of the initial atoms) is minimal at normal incidence and increases monotonically with increasing angle of incidence. When the angle of incidence is fixed, the energy reflection coefficient of deuterium atoms from copper decreases monotonically with energy from 300 eV to 160 keV. When a beam with energy of ~30 keV is incident at an angle of 54° to the normal (outermost plates), about 2% of the incident energy is reflected, and when a beam with energy of ~30 keV is incident at an angle of 82° (central plates), about 20% of the incident energy is reflected. Therefore, the reflection of energy at large angles of incidence can lead to a noticeable difference between the real normal power density and the calculated one.
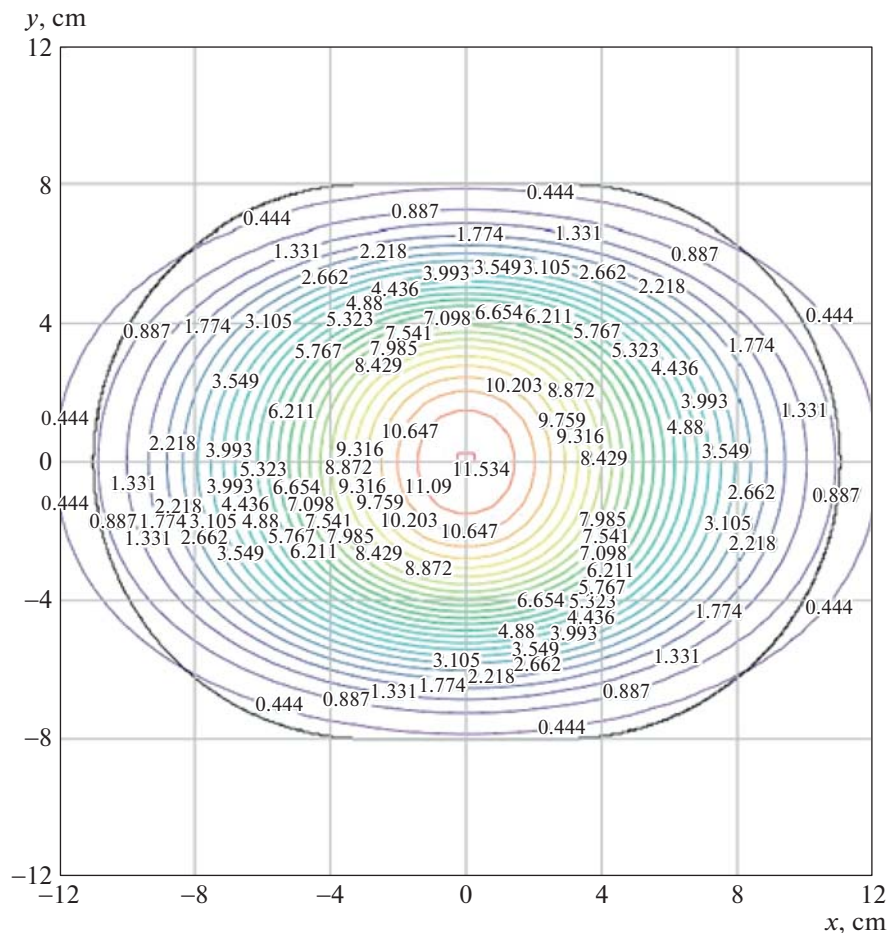
Fig. 3. Power density distribution in the beam at the RC diaphragm.

Another energy loss channel is sputtering of the plate material. However, for light beam atoms, the energy carried away by the sputtered target atoms is much less than the energy carried away by the reflected beam atoms. It follows from the calculated data [6] for energies of deuterium atoms up to 10 keV that the yield of copper atoms and the energy they carry away reach a maximum at energy of deuterium atoms of several keV and decrease with a further increase in energy. Therefore, we can take the energy of 3 keV for an upper estimate. Although the yield of copper atoms, which increases with the angle of incidence, is up to 30% at angles of incidence of about 80º, the energy carried away by these atoms is small and does not exceed 0.3% of the incident energy. Consequently, the energy loss for copper sputtering from the calorimeter plates can be neglected.

So, if the absorbed power of the outermost plates is almost equal to the incident beam power, then the local absorbed power of the central plates can be less than 80% of the incident power, taking into account the single reflection of the initial beam particles.

Design of Receiver Calorimeter

The receiver calorimeter has a sliding structure and consists of three main units (vacuum chamber with sighting device (diaphragm), right receiving panel, and left receiving panel). The layout of the device is shown in Fig. 5.

The vacuum chamber of the calorimeter is a welded structure. It provides a given spatial orientation of all its elements and is also part of the vacuum chamber of the beam path. The layout of the vacuum chamber with a diaphragm is shown in Fig. 6.

The sighting device (SD) is a soldered connection of two disks with a cooling tube soldered into one of them. One of the disks has space for the location of secondary emission sensors. The SD determines the spatial position of the beam at the entrance to the calorimeter and cuts off the beam halo. The layout of the SD is shown in Fig. 7.

The right and left receiving panels are located on opposite sides of the RC vacuum chamber and consist of several assembly units, which in combination provide a given spatial position of the receiving panel, its movement in vacuum, vacuum−atmosphere separa-

Table 1. Calorimeter thermocouple coordinates*

Parameter	Left side of the calorimeter					Right side of the calorimeter				
Upper thermocouples, $y = +30$ mm										
Plate number	9	7	5	3	1	2	4	6	8	10
Thermocouple number	05	06	07	08	10	20	18	17	16	15
Angle between the plate and y–z plane, degrees	36	20	12	9	8	8	9	12	20	36
Power density, kW cm^{-2} (calculation)	1.97	7.17	10.82	12.67	13.50	13.56	12.74	10.90	7.23	1.99
Normal power density P_n, kW cm^{-2} (calculation)	1.16	2.45	2.25	1.98	1.88	1.89	1.99	2.27	2.47	1.17
Lower thermocouples, $y = -30$ mm										
Plate number	9	7	5	3	1	2	4	6	8	10
Thermocouple number	01	02	03	04	09	19	14	13	12	11
Angle between the plate and y–z plane, degrees	36	20	12	9	8	8	9	12	20	36
Power density, kW cm^{-2} (calculation)	1.97	7.17	10.82	12.67	13.50	13.56	12.74	10.90	7.23	1.99
Normal power density P_n, kW cm^{-2} (calculation)	1.16	2.45	2.25	1.98	1.88	1.89	1.99	2.27	2.47	1.17

* The z coordinate is measured from the diaphragm at the calorimeter input ($z = 225.4$ cm from the grids of the ion optical system) in the direction of beam propagation; x coordinate is measured from the vertical beam symmetry plane; and y coordinate is the distance between the horizontal beam symmetry plane and the calorimeter plates (+30 mm and −30 mm).

tion, and connection to the pressure and drain lines. The layout of one of the receiving panels is shown in Fig. 8.

Each receiving panel has support elements that are both in a vacuum and in the atmosphere. In a vacuum, the unit is fixed between the guide rollers in a vertical plane and rests with its rollers on four brackets located on the cover of the vacuum chamber. In the atmo-sphere, the unit is fixed on the carriage guide. Rolling bearings are installed in all support elements of the unit. The suspension diagram of the receiving panel unit is shown in Fig. 9.

Electric drives move the panels. Movement in vac-uum is carried out through a bellows unit. The system for supplying and draining coolant is organized as a pipe-in-pipe and combined into a common water col-lector. It is a hermetic welded structure in which a
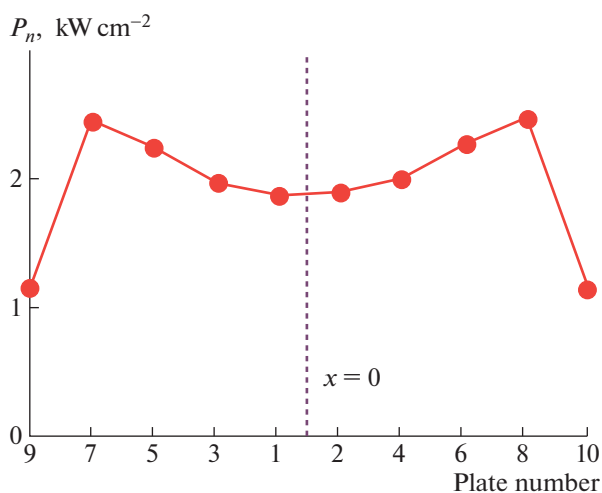

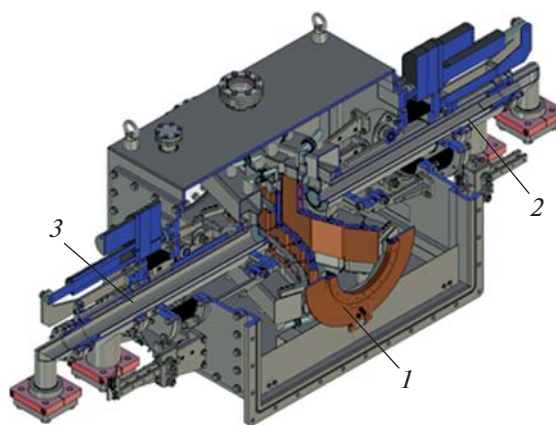**Fig. 4.** Calculated normal power density on the plates (see the last line of Table 1).

Fig. 5. Layout of the receiver calorimeter and its main ele-ments. (*1*) Vacuum chamber with sighting device (dia-phragm), (*2*) right receiving panel unit, and (*3*) left receiv-ing panel unit.

Table 2. Data on thermocouple temperature by levels (upper−lower) and sides (left−right)

Parameter	Left side of the calorimeter					Right side of the calorimeter				
Upper thermocouples, $y = +30$ mm										
Thermocouple number	05	06	07	08	10	20	18	17	16	15
Angle between the plate and the y−z plane, degrees	36	20	12	9	8	8	9	12	20	36
Measured temperature, °C	84/90	120/122	63/62	100/98	100/98	102/83	109/108	47/46	148/145	103/109
Lower thermocouples, $y = -30$ mm										
Thermocouple number	01	02	03	04	09	19	14	13	12	11
Angle between the plate and the y−z plane, degrees	36	20	12	9	8	8	9	12	20	36
Measured temperature, °C	87/90	127/129	59/58	92/94	92/94	107/104	93/98	68/67	131/132	93/91

smaller diameter pipe of 64 mm is located inside a larger diameter pipe of 90 mm. Water is supplied through the pipe of larger diameter, and water is drained through the pipe of smaller diameter. Appropriate elements that provide a tight connection to the water lines are welded at the end of each of the pipes. Such an arrangement greatly simplifies the design and allows the use of water collectors as motion-transmitting elements. The layout of the water collector is shown in Fig. 10.

Heat exchangers (receiving plates) and a support with which the unit moves in vacuum are attached to the water collector. The heat exchangers are attached to a support bracket, which is screwed to the water collector, and the connecting pipes are welded to the heat exchangers and the water collector. Each pipe branch

has a bellows insert to compensate for thermal deformations of the receiving plate during beam heating. The layout of the receiving panel is shown in Fig. 11.

The receiving panels are closed inside the vacuum chamber, forming a V-shaped receiver. This shape of the receiver makes it possible to obtain the smallest size along the beam axis [7], and the heat exchangers on each receiving panel are located at different angles with respect to the beam axis. The location at one angle is not required because the highest power density is at the center of the beam. This allows reducing the RC size. The angles of inclination of the heat exchangers with respect to the axis of motion of the particle beam are shown in Fig. 12.

All receiving plates are designed in the same way, with the exception of one, the edge of which is cham-
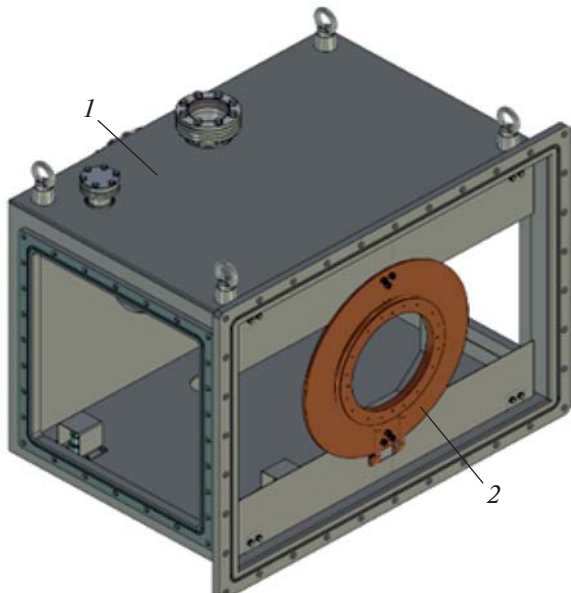

Fig. 6. Layout of the vacuum chamber with sighting device and its main elements. (*1*) Vacuum chamber and (*2*) sighting device (diaphragm).
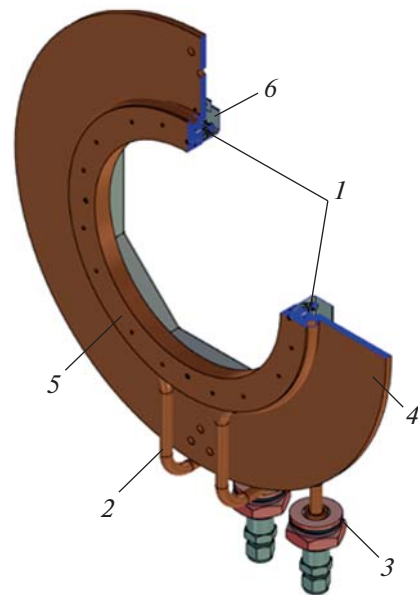

Fig. 7. Layout of the sighting device and its main elements. (*1*) Secondary emission sensors, (*2*) cooling tube, (*3*) vacuum−atmosphere decoupling, (*4*) disk, (*5*) sensor housing, and (*6*) shield.
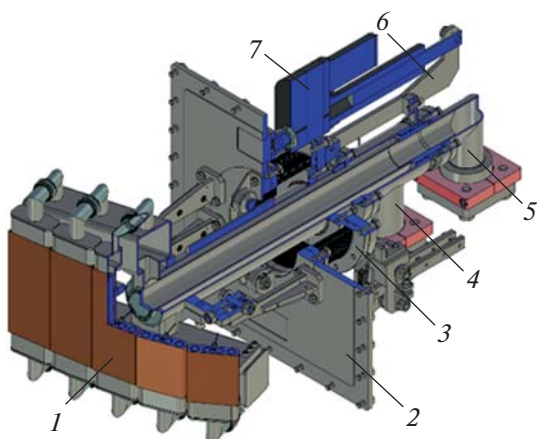
Fig. 8. Layout of the receiving panel assembly and its main elements (*1*). Receiving panel, (*2*) vacuum chamber cover, (*3*) bellows unit (vacuum−atmosphere decoupling), (*4*) water inlet pipe branch, (*5*) water outlet pipe branch, (*6*) pusher, and (*7*) electric actuator.
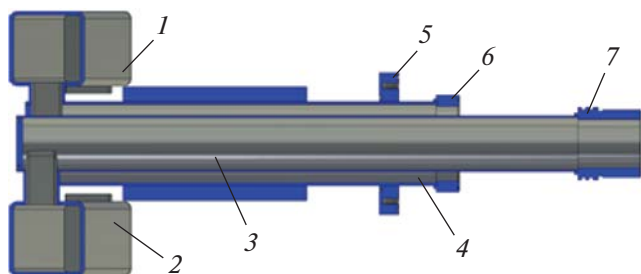

Fig. 9. Suspension system of the receiving panel unit. (*1*) Carriage guide (atmosphere), (*2*) guide roller, and (*3*) bracket.

Fig. 10. Layout of water collector and its main elements. (*1*) Inlet receiver collector, (*2*) outlet receiver collector, (*3*) outlet pipe, (*4*) inlet pipe, (*5*) vacuum−atmosphere decoupling flange, (*6*) connecting flange to the inlet line, and (*7*) connecting flange to the outlet line.

Fig. 11. RC receiving panel and its main elements. (*1*) Water collector, (*2*) heat exchanger support bracket, (*3*) support, (*4*) heat exchanger, and (*5*) connection pipe.

fered, closing the panels without a gap. This is done to overlap the beam. Each heat exchanger is a copper plate with a thickness of 22 mm having four channels, in which flow swirlers (heat transfer enhancers) are installed [2] (Fig. 13). The swirlers swirl the flow. The design includes a swirler formed by an insert completely blocking the channel with a single-start wire winding.

This type is not sufficiently effective in terms of heat transfer enhancement [2], since it completely covers the channel section, forming an annular channel of a slotted profile. However, this configuration has a number of advantages in terms of manufacturing technology and water mass flow. To measure the heating temperature of the plates and determine the beam profile, two thermocouples (TKhK-01) are installed on each of them. The end of the thermocouple is at a distance of 2 mm from the surface of the receiving plate. The end of the thermocouple is embedded in the
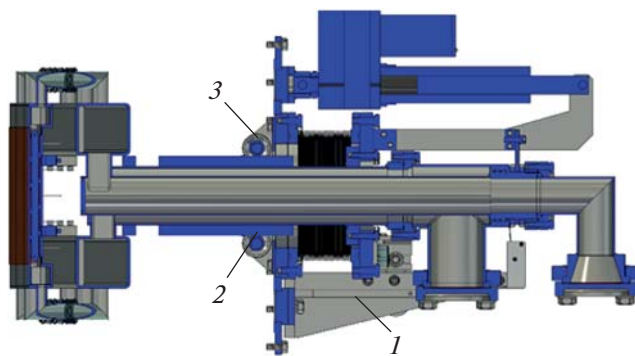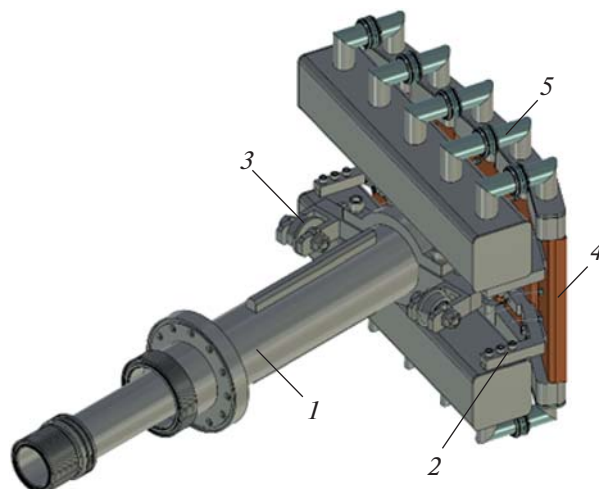
plate using indium−gallium−tin eutectic. The eutectic is in a liquid state at a temperature of 5−10°C. This provides thermal contact between the thermocouple and the panel receiving plate. The design of the heat exchanger is shown in Fig. 14.

Plates with swirlers located in them are quite sensitive to deformations, in particular, bending of the plate as a consequence of thermal expansion of the metal. Significant displacements lead to the destruction of the RC elements. The configuration of the thick plate with four combined channels has sufficient stiffness, part of which is provided by swirlers.

Thermal and Hydraulic Calculations of Calorimeter

All thermal and hydraulic calculations were carried out using the ANSYS program [8] in the Fluent and Mechanical environments. First of all, a hydrodynamic calculation of the movement of the coolant in
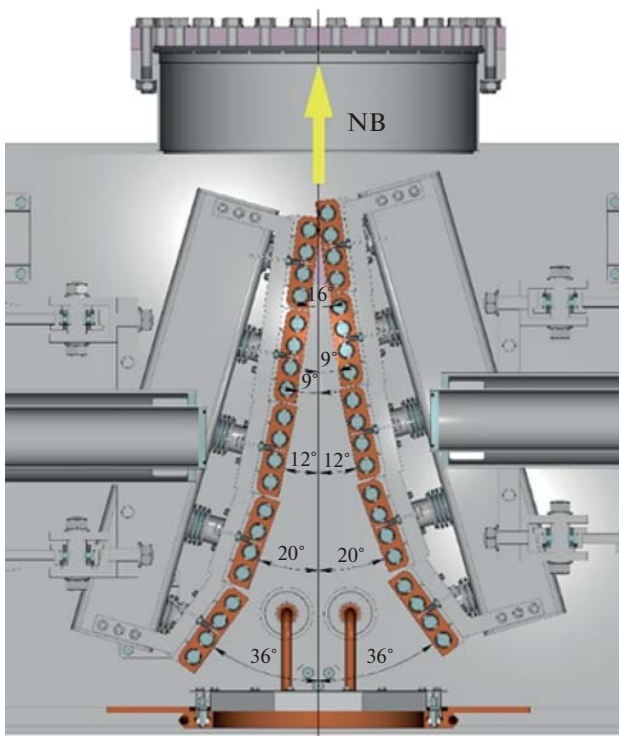
Fig. 12. Inclination angles of heat exchangers.

the RC hydraulic system was made. The flow pressure at the system inlet (6 atm) was taken as the initial design parameter. This formulation of the problem made it possible to estimate the correctness of the chosen hydraulic scheme and to determine some values of the flow motion parameters. The flow rates in all zones of the water path for this mode are calculated; the required fluid flow is determined; the places of the coolant reverse flow and flow swirl and stagnant zones are identified. The optimization was carried out using the data. Calculation of the liquid flow rates in the water line of the calorimeter corresponding to the flow rate of 700 L min⁻¹ is shown in Fig. 15. The water pressure drop in the system is shown in Fig. 16. The water

pressure at the inlet is 600 kPa (6.1 atm), and the water pressure at the outlet is 11 kPa (0.1 atm).

The next step was to calculate the conjugate heat transfer of the receiving plate in the Fluent environment. This method of calculation makes it possible to simulate the mode of beam power absorption by a receiving plate cooled by a coolant. The model of the receiving plate for the calculation was as close as possible to the real model, with the exception of some simplifications. The initial parameters of the calculation were water velocity at the inlet to the heat exchanger ($V = 6$ m s⁻¹) and the power density incident (absorbed) on the plate, which was set in accordance with the calculation of the power density distribution in the beam. According to the power density distribution in the beam, the load on the plate decreases from the center to its edges. To simplify calculations, the plate surface was divided into four load zones. The load distribution on the plate is shown in Fig. 17.

The red zone corresponds to the maximum value of power density (1.88 ± 0.04 kW cm⁻²); the brown zone corresponds to 1.30 ± 0.04 kW cm⁻²; the yellow zone corresponds to 0.88 ± 0.04 kW cm⁻²; and the green zone corresponds to 0.35 ± 0.04 kW cm⁻².

Thus, there are four zones on the receiving plate; each of the zones is characterized by its own power density.

Heating of water in the channels of the plate averaged 32°C. The pressure drop was 3.6 atm, and the mean heat transfer coefficient of water near the surface of the cooling channels was 8×10^4 W (m² K)⁻¹ on average. The time dependence of the surface temperature of the plate absorbing the beam power is shown in Fig. 18.

The calculated mass flow rate for this temperature mode was 2.5 kg s⁻¹ per heat exchanger. Thus, the flow rates per second and minute per one receiving panel are 12.5 L s⁻¹ and 750 L min⁻¹, respectively. Such water consumption provides sufficient heat removal, at which there are no destructive thermal deformations for the elements of the calorimeter. Although the
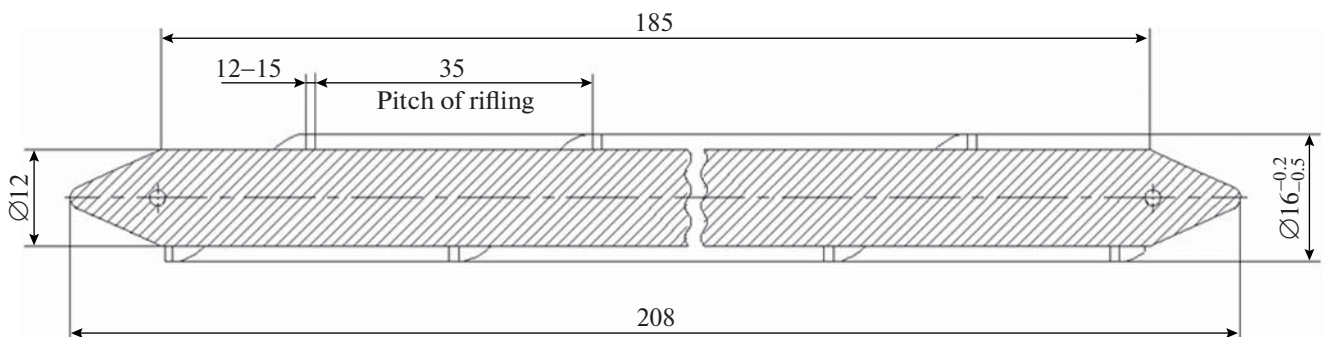

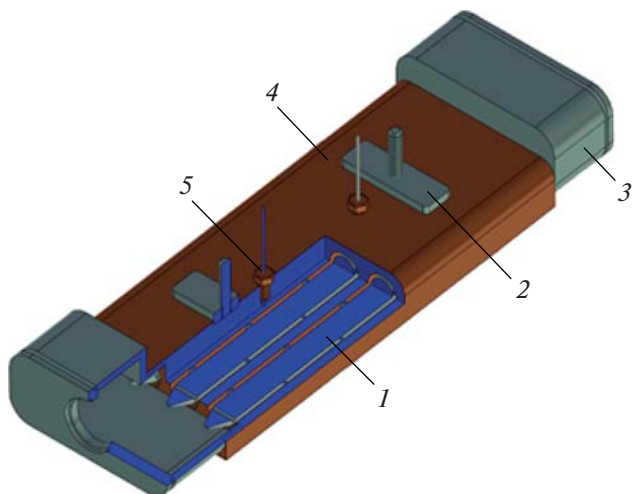**Fig. 13.** Design and main size of the swirler.

Fig. 14. The design of the RC heat exchanger and its main elements. (*1*) Swirl (heat exchanger), (*2*) support plate, (*3*) receiver cap, (*4*) receiving plate, and (*5*) thermocouple.

significant rigidity of the plate with the swirlers makes it possible to resist bending, when the temperature reaches 700°C and above, the heat exchanger will be subject to a rather complex deformation. In general, most of the heat exchanger will be quite cold, and a strongly heated surface layer with a thickness of 2–4 mm will expand both in the axial direction and in the transverse direction. Movements of a few millimeters will lead to a possible loss of tightness of welded and soldered joints. In addition, the expanded copper layer will put a lot of pressure on the steel swirler, which can destroy it.

For comparison, we present the data on water consumption on the calorimeters of some injectors in the megawatt range. In [9], a calorimeter with a pressure drop of 10 atm and a mass flow rate of water of about 2000 L min^{-1} was used for a PINI injector on TEXTOR; in [10], a calorimeter with water pressure drop of 11.5 atm and the total mass flow rate of water of about 2500 L min^{-1} was used for an injector with a power of 3 MW at the METF unit; in [11], a calorimeter with a mass flow rate of 300 L min^{-1} was used for an injector with a power of 1 MW and a duration of 1 s. In [12], the mass flow rate of the tokamak calorimeter of the National Research Center Kurchatov Institute for an injector with a power of 3.7 MW in atoms is 30 L s^{-1} at 8 atm.

TCV Operating Experience

The atom injector has been operating at the TCV in Lausanne since 2015. During this time, the calorimeter underwent about 1000 shots at different beam powers and pulse durations. During the operation, the cal-
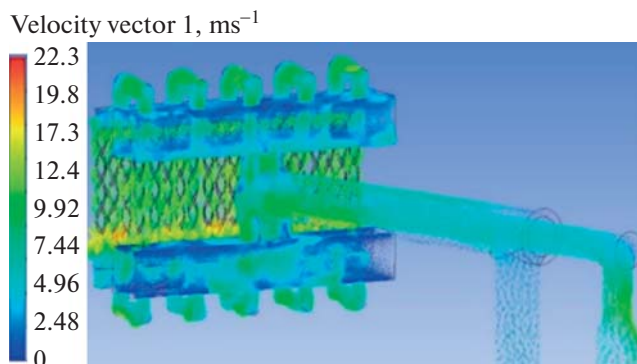

Fig. 15. Velocity vectors of fluid flow in the water line of the calorimeter.

orimeter did not require any service work or replacement of any components.

During the operation of the TCV atom injector, temperature data were obtained from the thermocouples of the receiving plates of the calorimeter. The measurements were carried out at a neutral beam power of 1.30 MW and pulse duration of 500 ms; water flow per panel was 420 L min^{-1}, and flow pressure at the inlet was 3.3 atm. Table 2 shows temperature data on thermocouples by levels (upper–lower) and sides (left–right).

Figure 19 shows the measured experimental temperature data on thermocouples (divided into four zones).

The response time to the beam for thermocouple 7 (plate 5 of the left side of the calorimeter) and thermocouples 17 and 13 (plate 6 of the right side of the calorimeter) was $\tau \sim 1.3$ s, which is 2.6 times longer. This negative factor can be explained as follows. Since all the plates of the calorimeter are the same, this apparently means that, for thermocouples with a long characteristic temperature settling time, the thermal con-
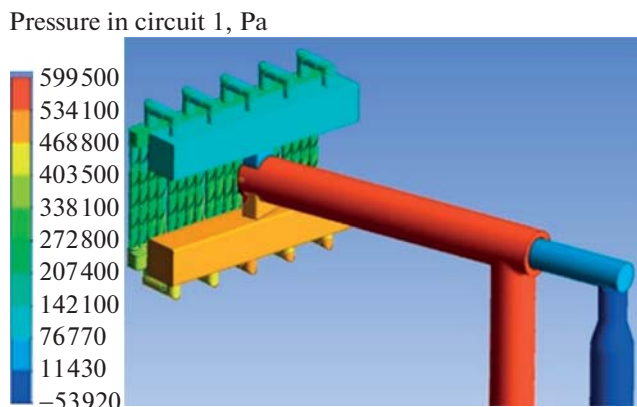

Fig. 16. Drop in water pressure in the water line of the calorimeter.

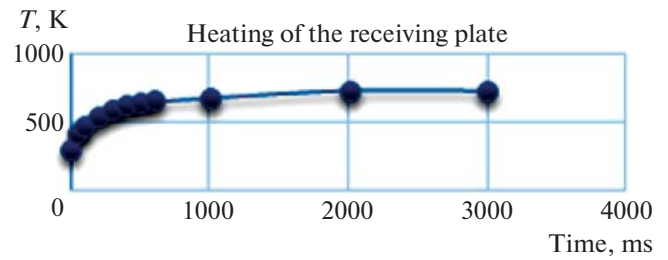**Fig. 17.** Beam power density distribution on a plate.

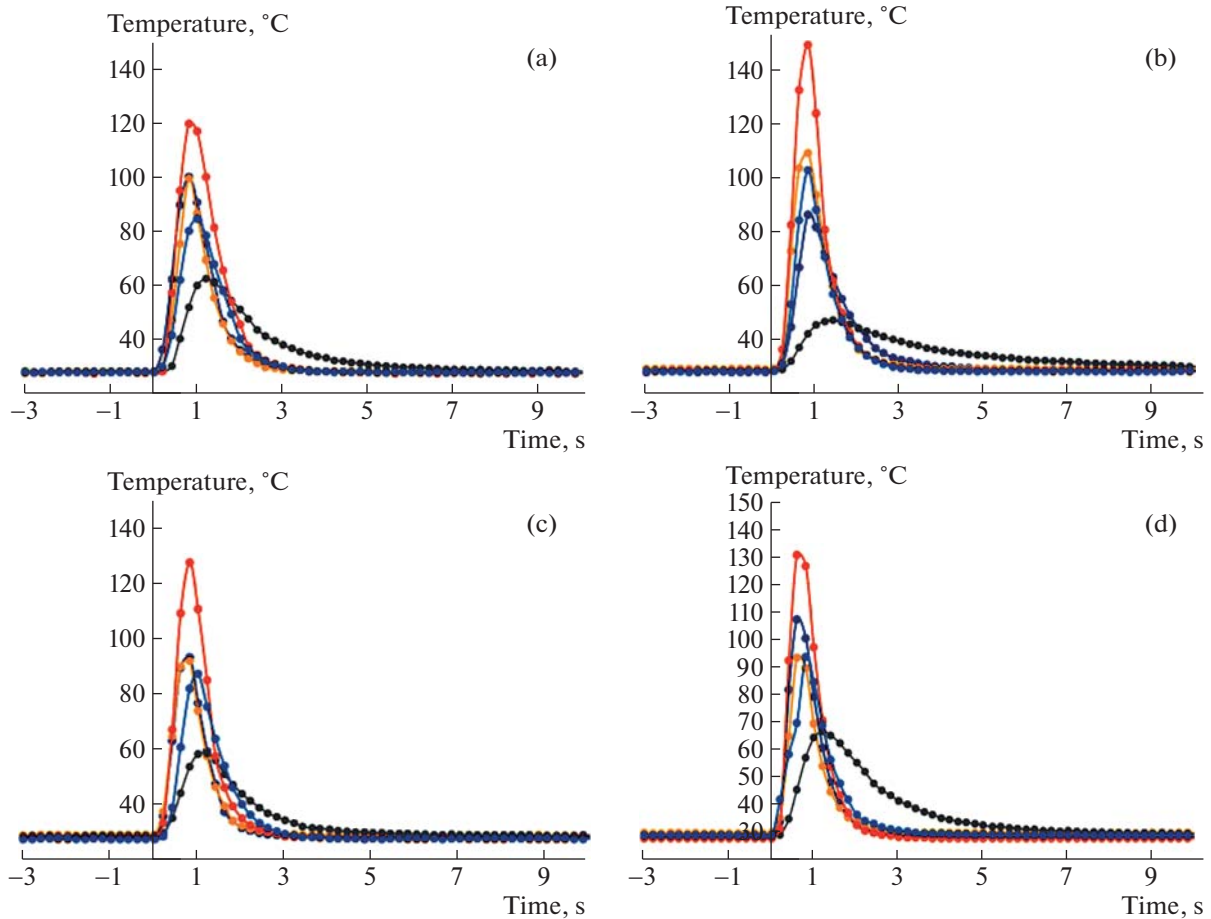**Fig. 18.** Time dependence of temperature of the receiving plate.

Fig. 19. Time dependence of temperature for thermocouples nos. 1−20. (a) Upper left calorimeter ((●) TC 10, (●) TC 8, (●) TC 7, (●) TC 6, and (●) TC 5); (b) upper right calorimeter ((●) TC 20, (●) TC 18, (●) TC 17, (●) TC 16, and (●) TC 15); (c) lower left calorimeter ((●) TC 9, (●) TC 4, (●) TC 3, (●) TC 2, and (●) TC 1); and (d) lower right calorimeter ((●) TC 19, (●) TC 14, (●) TC 13, (●) TC 12, and (●) TC 11).

tact between the plate and the thermocouples is weak (low thermal diffusivity of the contact) and does not ensure fast temperature setting of the thermocouple in accordance with the temperature of the plate in this region. Therefore, temperature measurements by thermocouples 7 and 3 (plate 5 of the left side of the calorimeter) and thermocouples 17 and 13 (plate 6 of the right side of the calorimeter) should be excluded from the analysis.

CONCLUSIONS

The calorimeter described in this work was put into operation in 2015. It withstood more than 1000 shots with a beam power of more than one megawatt during its operation in autonomous modes. The receiver calorimeter absorbed both full-pulse beams and modulated beams. The calorimeter systems operated properly all the time.

The design of the RC has undergone a number of technical solutions, such as receiving plates with liquid flow swirlers installed in them to enhance heat transfer and water supply and pipe-in-pipe collectors of water inlet and water outlet introducing movement into a vacuum, which made it possible to achieve high energy efficiency at relatively low costs of coolant, small overall dimensions of the device, relatively low weight of the device, modular design, ease of assembly, adjustment, maintenance, and ease of manufacture of calorimeter elements.

ACKNOWLEDGMENTS

CONFLICT OF INTEREST

REFERENCES

1. A. N. Karpushov, R. Chavan, S. Coda, et al., Fusion Eng. Des. **123**, 468 (2017).
2. O. V. Mitrofanova, *Hydrodynamics and Heat Transfer of Swirling Flows in the Channels of Nuclear Power Plants* (Fizmatlit, Moscow, 2010) [in Russian].
3. A. V. Sorokin, T. D. Akhmetov, A. V. Brul, V. I. Davydenko, A. A. Ivanov, A. N. Karpushov, V. V. Mishagin, and I. V. Shikhovtsev, Rev. Sci. Instrum. **91**, 013323 (2020).
4. T. D. Akhmetov, V. I. Davydenko, and A. A. Ivanov, IEEE Trans. Plasma Sci. **36**, 1545 (2008).
5. W. Eckstein, Report IPP 17/12 (Max-Planck-Inst. Plasmaphysik, 2009). http://pubman.mpdl.mpg.de/pubman/item/escidoc:2141005/component/escidoc:2141004/IPP_report_17_12_Eckstein.pdf.
6. W. Eckstein, Report IPP 17/29 (Max-Planck-Inst. Plasmaphysik, 2009). http://pubman.mpdl.mpg.de/pubman/item/escidoc:2140248/component/escidoc:2140247/IPP_17_29.pdf.
7. Yu. I. Belchenko and V. I. Davydenko, et al., Phys. Usp. **61**, 531 (2018).
8. ANSYS Workbench Platform. http://www.ansys.com.
9. H. Euringer, M. Lochter, U. Pfister, and R. Uhlemann, in *Proceedings of IEEE 13th Symposium on Fusion Engineering, Knoxville, TN, 1989,* Vol. 2, p. 992.
10. S. K. Combs, S. L. Milora, C. A. Foster, H. H. Haselton, M. M. Menon, and C. C. Tsai, Rev. Sci. Instrum. **56**, 1526 (1985).
11. A. Sorokin, V. Belov, V. Davydenko, P. Deichuli, A. Ivanov, A. Podyminogin, I. Shikhovtsev, G. Shulzhenko, N. Stupishin, and M. Tiunov, Rev. Sci. Instrum. **81**, 02B108 (2010).
12. V. K. Naumov and N. N. Semashko, Vopr. At. Nauki Tekh., Ser.: Termoyad. Sintez, No. 1 (5), 67 (1980).

Translated by I. Obrezanova

SPELL OK